View metadata, citation and similar papers at core.ac.uk

brought to you by CORE

provided by KITopen

Received: 3 June 2020 | Revised: 12 July 2020 | Accepted: 12 July 2020

DOI: 10.1002/jrs.5953

Check for updates

RESEARCH ARTICLE

Journal of RAMAN SPECTROSCOPY WILEY

Short-range ordering in the Li-rich disordered rock salt cathode material Li_2VO_2F revealed by Raman spectroscopy

Nataliia Mozhzhukhina[1] | Jolla Kullgren[1] | Christian Baur[2] | Olof Gustafsson[1] | William R. Brant[1] | Maximilian Fichtner[2,3] | Daniel Brandell[1]

[1]Department of Chemistry—Ångström Laboratory, Uppsala University, Uppsala, Sweden

[2]Helmholtz Institute Ulm, Ulm, Germany

[3]Institute for Nanotechnology, Karlsruhe Institute of Technology, Karlsruhe, Germany

Correspondence
Nataliia Mozhzhukhina, Department of Chemistry—Ångström Laboratory, Uppsala University, Box 538, SE-751 21 Uppsala, Sweden.
Email: nataliia.mozhzhukhina@kemi.uu.se

Funding information
European Union's Horizon 2020 research and innovation program, Grant/Award Number: 711792 (LiRichFCC); STandUP for Energy; Swedish National Infrastructure for Computing (SNIC)

Abstract

Li-rich disordered rock salt (DRS) materials are new promising high-capacity cathode candidates for Li-ion batteries. DRS structures were initially assumed to have a completely random cation and anion distribution, but recent reports suggest that some of these structures can exhibit local atomic arrangements, or short-range ordering (SRO). Here, we prove the existence of SRO in the Li-rich DRS material Li_2VO_2F by employing Raman spectroscopy supported by density functional theory (DFT) calculations. Our results suggest that this combination of Raman spectroscopy with computational tools is useful for SRO estimation in this new class of Li-rich DRS cathode materials.

KEYWORDS

anionic redox, DFT calculation, disordered rock salt, Li-ion battery, short-range ordering

1 | INTRODUCTION

There is an ongoing search for novel Li-ion battery cathode materials which possess a high energy density, while employing more available, cheaper, and less toxic elements than the conventional Co-based materials.[1] Li-rich disordered rock salt (DRS) materials are able to cycle reversibly more than one lithium ion per transition metal (TM) and are thereby among the most attractive candidates for this purpose.[2–4] This category of materials is characterized by crystalline face-centered cubic rock salt structures, in which the oxygen and fluorine anions stack to form a face centered cubic arrangement with the transition metal and lithium cations randomly occupying all the octahedral interstitial sites. Substituting some oxygen atoms by fluorine can trigger a lower oxidation state of the TM, leading to higher lithium content, and consequently to an increased energy density.[5–7] One example in this class of materials is the Li-rich DRS Li_2VO_2F, which was introduced by Chen et al.[3] This fairly novel cathode material features a 1.8 Li^+ capacity per TM, corresponding to 420 mAh/g (in comparison to 280 mAh/g for the standard $LiCoO_2$ electrode), at an average potential of 2.5 V versus Li^+/Li. However, the Li_2VO_2F cathode has been shown to suffer from irreversible degradation reactions and fading capacity.[8,9] In order to mitigate these instabilities, the structure-dynamic properties of the material during battery operation must be better elucidated.

Notably, X-ray diffraction (XRD) remains one the most commonly employed experimental tools for crystal structure determination of Li-rich materials, with the

This is an open access article under the terms of the Creative Commons Attribution License, which permits use, distribution and reproduction in any medium, provided the original work is properly cited.
© 2020 The Authors. Journal of Raman Spectroscopy published by John Wiley & Sons Ltd

widely agreed assumption that the cations and anions are randomly distributed on their respective sites in the structure. However, it is known that although XRD generally reveals the long-range average crystalline structure of the material, the short-range order (SRO) mainly remains hidden in the powder-based diffraction data analyzed by Rietveld methods. Another diffraction limitation comes from the fact that F and O have the same X-ray scattering length and are therefore impossible to distinguish. It has recently been revealed that a cation SRO is present in several DRS materials and that this can have a significant impact on the transport properties and electrochemical performance.[10–13] The SRO has previously been studied by a combination of experimental (electron diffraction [ED],[10] solid state nuclear magnetic resonance [NMR],[11,13] and 2D and 3D nanoscale X-ray spectro-microscopy[12]) and theoretical methods (DFT and molecular dynamics [MD] simulations). As pointed out in a recent review by Clément et al.,[2] fluorine substituted DRS are extremely difficult to characterize by classical experimental techniques such as X-ray absorption spectroscopy (XAS), X-ray, or neutron diffraction, whereas F^{19} NMR, in contrast, is emerging as a useful tool to characterize the anion sites in DRS.

Raman spectroscopy is a well-known tool that is often used to complement XRD when characterizing the crystalline structure of a material. This is not least due to the fact that, unlike XRD Rietveld analysis, Raman spectroscopy is more sensitive to the SRO in a crystal.[14,15] However, to the best of our knowledge, there are currently no studies employing Raman spectroscopy in order to reveal SRO in Li-rich DRS cathodes. Here, we employ Raman spectroscopy, supported by DFT calculations, for studying the SRO in the Li_2VO_2F material, which is a relevant example of both a cation and anion disordered Li-rich disordered rock salt structure.

2 | EXPERIMENTAL DETAILS

The Li_2VO_2F cathode material was synthesized following a high energy ball milling procedure as described elsewhere.[9,16] All steps were either conducted in a glovebox under argon atmosphere (water and oxygen levels below 0.1 ppm) or in sealed vials under argon atmosphere. V_2O_3 (Alfa Aesar, 99.7%), Li_2O (Alfa Aesar, 99.7%), and LiF (Alfa Aesar, 99.9%) were used as precursor materials.

The chemically delithiated samples of Li_xVO_2F were synthesized using Schlenk-line-techniques under argon atmosphere. For the chemical delithiation, ½ I_2, 1 I_2, or 1 Br_2 in stoichiometric amounts with respect to Li_2VO_2F was used, assuming a complete conversion. Stoichiometric quantities of each halogen were added to a suspension of Li_2VO_2F in acetonitrile (Merck, <10 ppm H_2O) and stirred for 1 week at room temperature to facilitate a homogenous extraction of Li. Subsequently, the residual Li_xVO_2F powder was filtered and washed multiple times with acetonitrile to remove residual LiI or LiBr, respectively. The Li-content of the delithiated samples was determined using an inductively coupled plasma optical emission spectrometer (ICP-OES), by Medac Ltd. Based on the ICP-OES results, the Li_xVO_2F stoichiometry was determined as follows: $Li_{1.2}VO_2F$ for the sample delithiated with ½ I_2, $Li_{1.15}VO_2F$ for the sample delithiated with 1 I_2, and $Li_{0.96}Li_2VO_2F$ for the sample delithiated with 1 Br_2.

Raman measurements on the Li_2VO_2F and Li_xVO_2F powders were performed in custom-made air-tight cells under argon atmosphere. All Raman spectra were measured under an argon atmosphere utilizing three lasers with different excitation wavelengths (532, 633, and 784 nm), with a varying laser power and 400 s acquisition time, using a Renishaw inVia confocal Raman spectrometer equipped with a CCD camera and Leica LM optical microscope, utilizing a 50× long focus lens magnification. A grating of 1,800 lines/mm grove density has been used for the 532 and 633 nm and 1,200 lines/mm for the 784 nm laser excitation wavelength. A complete overview of the measurements can be found in Figures S1–S4.

The DFT calculations presented in this work were performed using the plane wave basis set and pseudopotentials code Vienna ab initio simulation package (VASP).[17–20] The exchange correlation energy was described using the Perdew–Burke–Ernzerhof (PBE[21,22]) functional. We applied a Hubbard correction of 3.25 eV to the d-electrons of vanadium using the rotational invariant DFT + U method by Dudarev et al.[23] Core electrons and the core-valence electron interactions were described with the pseudopotential and the projector augmented wave (PAW) method.[24]

All structures were optimized until the maximum forces on all atoms and the stress in the cell were below 0.01 eV/Å and 0.01 kbar, respectively. In all simulations, a Gaussian smearing of 0.025 eV for the electronic states was used. Raman intensities were obtained using VASP and a python-tool.[25] Vibrational modes were visually inspected using the Jmol software, and crystal structures were visualized using VESTA software.[26] Peak fitting was performed using MATLAB.

3 | RESULTS AND DISCUSSIONS

3.1 | Fully lithiated Li_2VO_2F

Rietveld refinement of powder neutron and X-ray diffraction patterns is a commonly used tool to determine the crystal structure of the target electrode material, including the Li-rich DRS materials. Li_2VO_2F diffraction patterns have been published before[3,9,27] and provide evidence that it is a face-centered cubic rock salt structure (space group *Fm-3 m*), with Li^+ and V^{3+} occupying *4a*, and O^{2-} and F^- occupying *4b* Wyckoff sites. It was originally assumed that both anions and cations are distributed completely randomly, as depicted in Figure 1a. However, it is important to keep in mind that the diffraction patterns provide information on the average long-range structure, whereas the features arising from local arrangements can often be lost with conventional diffraction analysis techniques. Raman spectroscopy can therefore be considered a complimentary tool to XRD that provides additional information on the local structural symmetries.

Raman normal modes depend on the geometrical arrangements of ions and can be predicted based on the crystallographic symmetry and the factor group analysis. The Bilbao crystallographic server[28] provides nuclear site analysis based on the space groups and the Wyckoff sites occupied by ions. From the crystallographic parameters estimated for Li_2VO_2F, with an assumption that cations and anions are randomly distributed, the structure should not possess any Raman active modes. This, however, is in stark contrast to the experimentally recorded spectrum, shown in Figure 2. The Raman spectrum obtained for Li_2VO_2F possesses two very broad peaks at around 650 and 800 cm^{-1}, whereas the sharp spike at around 610 cm^{-1} is an artifact attributed to the cosmic rays hitting the CCD detector. The peak broadness may result from the disordered nature of the material and also partly from the presence of an amorphous phase. Notably, when applying high laser power, the Raman signature of the compound changes dramatically and resembles that of Li_2VO_3,[5] Figures S1–S3. This effect is well known, as unstable materials tend to change their

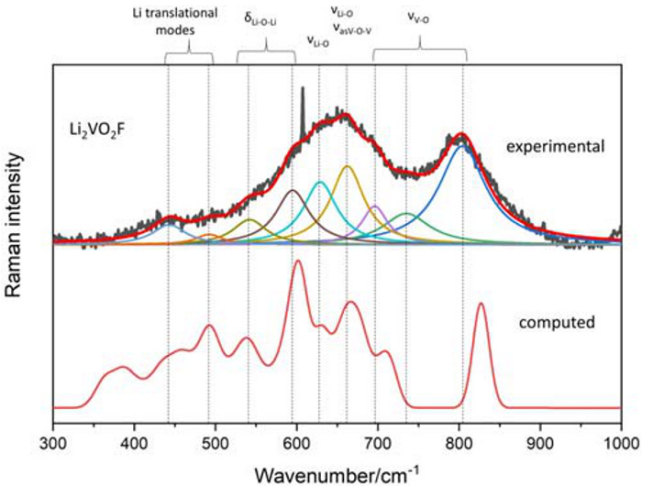

FIGURE 2 Experimental and computed Raman spectra of Li_2VO_2F

structures to more thermodynamically favorable configurations when subjected to high laser powers.[29] Because many of the DRS materials are metastable,[30] caution must be taken in order to avoid laser-induced structural transformations. The comparison between three distinct laser excitation wavelengths reveals that the use of the 785-nm laser provides the best resolved Raman spectrum of Li_2VO_2F under the maximum permittable laser power, Figure S4. Thereby, it can be suggested that this could be due to the electronic resonance effect, that is, that certain Raman intensities are enhanced when the laser excitation wavelengths approach the energy of electronic transition of the material.[31]

The reason behind the disparity between experimental results and those predicted by nuclear site analysis is that the local structural symmetry of Li_2VO_2F is different from that predicted by mentioned analysis. This suggests that the experimental Raman signature of Li_2VO_2F is an indication of the SRO. The introduction of distinct local symmetries due to SRO introduces additional modes activities, which could be both IR and Raman active. In this case, a more rigorous interpretation of the spectra can be achieved using theoretical simulations. We have therefore simulated Raman spectra of a number of Li_2VO_2F structures using DFT.

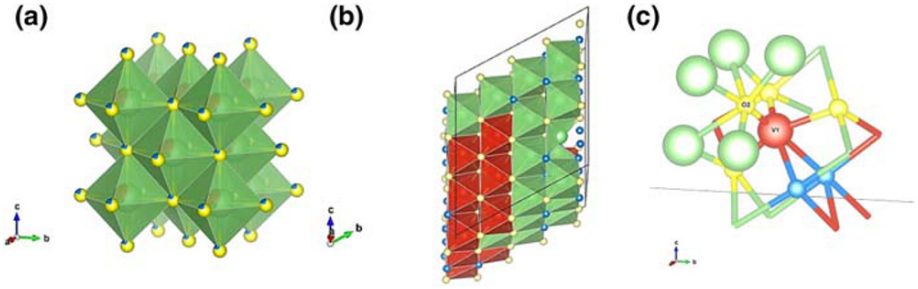

FIGURE 1 Schematic crystal structure representations of (a) Li_2VO_2F disordered structure with cations and anions distributed randomly; (b) Li_2VO_2F simulated crystal structure exhibiting local short-order arrangements; (c) local motive in the simulated Li_2VO_2F structure. Green, Li^+; red, V^{3+}; yellow, O^{2-}; and blue, F^-

Therefore, a 96 atoms supercell has been used to describe Li_2VO_2F. Representative structures were selected from a set of 64 structures with cations and anions randomly distributed on their respective sites in the structure. From this set, the eight most stable structures were selected, and their Raman spectra were subsequently simulated.

These simulated Li_2VO_2F structures were characterized by a variety of Raman active peaks in the 400 to 800 cm^{-1} wavenumber interval; however, only three out of eight most stable structures had Raman active bonds in the wavenumber region at or above 800 cm^{-1}. According to the DFT simulations, these higher wavenumber peaks are related to a local V–O oscillator, akin to an embedded molecular stretching vibrational mode within the crystal. Out of three, the Li_2VO_2F structure that we consider displays the most representative simulated Raman spectrum is shown in Figure 1b, and the corresponding Raman spectrum is depicted in Figure 2. The experimental Raman spectrum was fitted with nine Lorentzian peaks according to the active Raman modes predicted by DFT, with a reasonably good match (below 20 cm^{-1}) between computed and experimental peaks positions. A perfect match between the computed and measured Raman spectra cannot be expected due to several reasons. First, all exchange-correlation functionals within the applied DFT framework are approximate and hence lead to small errors in the calculated energies and forces. This, in turn, leads to small shifts in the Raman spectra, on the order of 10–30 cm^{-1}. Second, the thermal expansion of the crystal structure is not considered in the calculations. The lower wavenumber peaks are associated with Li translational modes and Li–O vibrations, whereas higher wavenumber peaks primarily are attributed to V–O vibrations. The three Raman bands at 804, 735, and 696 cm^{-1} can be assigned to V–O stretching vibrations, whose exact position shifts as a function of the V and O local environments. For example, as mentioned, the origin of the highest wavenumber band at above 804 cm^{-1} is due to the stretching vibration of a V–O bond, corresponding to a particular local environment. In this local structural motive (shown in Figure 1c), oxygen is surrounded by five lithium neighbors and one vanadium, whereas vanadium has four oxygen neighbors and two fluorine neighbors. It is worth mentioning that this special motive appears at the interphase between a Li-rich and V-rich region in the structure. Experimental and computed Raman peaks positions and their assignments are listed in Table S1. Notably, the assigned modes are in good agreement with results presented in literature both for the lithium involved modes[32,33] and V–O stretching modes.[34]

The simulated structure of Li_2VO_2F possesses very specific local ionic SRO that affects the arrangements of both the cations (lithium and vanadium) and anions (oxygen and fluorine). These effects can be seen from the histograms depicting the anionic and cationic environments, shown in Figure 3.

For a completely random anion distribution in Li_2VO_2F, each cation (independently whether it is Li^+ or

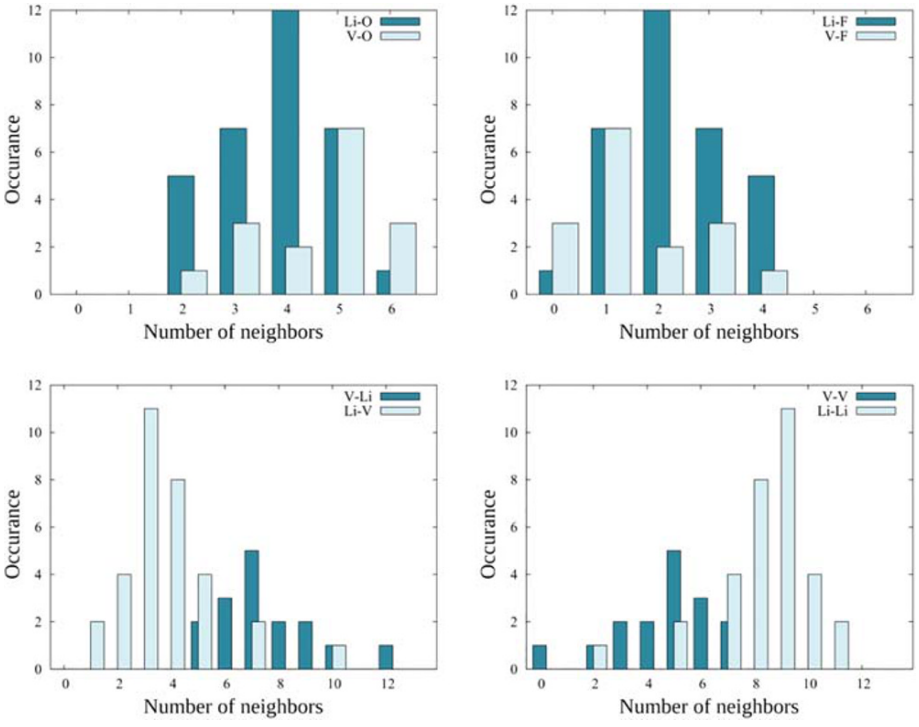

FIGURE 3 Histograms showing the anionic environments and cationic closest neighbors of Li^+ and V^{3+} in the Li_2VO_2F simulated structure

V^{3+}) will be surrounded by four oxygen and two fluoride anions on average. In other words, the number of oxygen neighbors for both Li^+ and V^{3+} should be two times higher than the number of fluoride neighbors. However, for the chosen simulated Li_2VO_2F configuration, the number of oxygen neighbors around Li^+ is only 1.25 times higher than the number of fluorine neighbors, whereas for V^{3+}, the number of oxygen neighbors is three times higher than the number of fluorine neighbors. It can be concluded that Li^+ ions are preferentially surrounded by F^-, whereas V^{3+} have more probability to be surrounded by O^{2-} rather than F^-.

A similar analysis can be done in order to evaluate the cationic SRO. In a completely random Li_2VO_2F structure, each cation, V^{3+} or Li^+, should have a total of 12 closest cation neighbors, eight of which are lithium and four of which are vanadium. That is, each cation will have two times more Li^+ neighbors than V^{3+} neighbors. However, the average number of Li^+ neighbors around Li^+ is 2.2 times higher than the number of V^{3+}, whereas for vanadium, this number is 1.6. Therefore, it can be concluded that the crystal structure possesses V-rich and Li-rich regions, rather than a uniform random distribution of cations. It is worth mentioning that other stable simulated structures (not shown) also exhibited similar localized anionic and cationic arrangements.

3.2 | Delithiated Li_2VO_2F

When Li_2VO_2F is employed as a cathode in a Li-ion battery, the delithiation or charging occurs according to the following reaction:

$$Li_2VO_2F \rightarrow xLi^+ + xe^- + Li_{2-x}VO_2F.$$

Chen et al.[3] have reported an extraction of 1.8 Li^+ per TM upon charging, which indicated that a complete delithiation to Li_0VO_2F is not feasible. This is also in agreement with the work performed by Whittingham et al.,[35] who suggest that a complete delithiation to VO_2F (space group R-3c. No. 167) is unlikely, and instead the material maintains its original DRS structure during the incomplete delithiation.[35]

Here, the Raman signature of the pure and chemically delithiated Li_xVO_2F cathode material has been analyzed. Electrochemical delithiation would involve preparing the slurry with only 70% *w*/w of active material (and 20% w/w carbon black and 10% w/w polyvinylidene fluoride (PVDF) binder), which in turn would seriously decrease the quality of the Raman data and complicate the analysis. The main purpose of the current work is to understand the Raman spectra of pristine lithiated and delithiated Li_xVO_2F, and therefore, chemical rather than electrochemical delithiation was chosen. Further, in situ Raman analysis is also complicated by the nanostructured morphology of the material, which makes it very challenging to focus on a single Li_2VO_2F particle via confocal Raman spectroscopy.

Raman spectra of three chemically delithiated Li_xVO_2F (with x equal to 1.2, 1.15, and 0.96) samples can be found in Figure S5. The experimental Raman spectrum of fully lithiated Li_2VO_2F, chemically delithiated $Li_{0.96}VO_2F$, and the simulated spectrum of VO_2F are shown in Figure 4. Because neither chemical nor electrochemical delithiation of Li_2VO_2F lead to a complete delithiation and formation of VO_2F, the experimental spectrum of this counterpart is not provided.

As expected, the Raman spectrum of $Li_{0.96}VO_2F$ is significantly affected by the delithiation. Most notably, the broad lower wavenumber peak at around 650 cm^{-1} that was attributed to Li translation modes and Li–O vibrations disappears. On the other hand, the higher wavenumber peak at around 800 cm^{-1}, associated with several V–O stretching vibrations, remains, whereas another very broad peak around 870 cm^{-1} evolves. The simulated VO_2F spectrum is characterized by one high wavenumber peak at 928 cm^{-1} and can only partly contribute to the delithiated $Li_{0.96}VO_2F$ spectrum. This result indicates that Li_2VO_2F maintains its general structure upon delithiation and does not undergo any complete conversion to Li_0VO_2F, much in agreement with previous reports.[3,35] The new Raman bands centered at 870 cm^{-1} could be explained by a combination of the V–O stretching mode shifts upon delithiation and the characteristic peroxide O–O vibration. The peroxide O–O peak

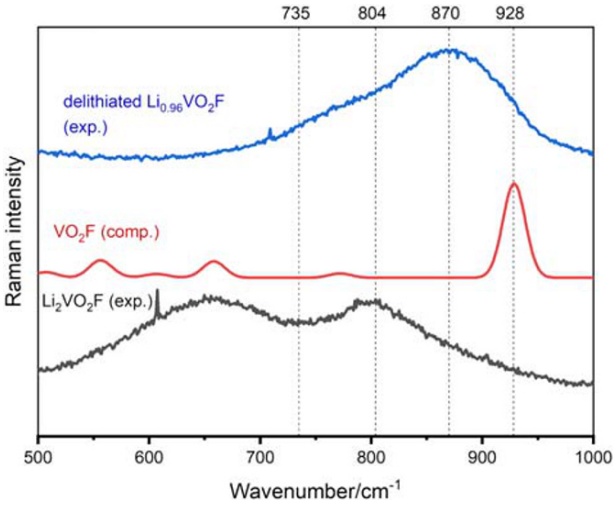

FIGURE 4 Experimental Raman spectra of a completely lithiated and chemically delithiated $Li_{0.96}VO_2F$; computed Raman spectrum of VO_2F

is expected to appear in the 800–900 cm^{-1} interval and has earlier been reported at 850 cm^{-1} during charging of Li-rich rock salt cathodes.[36,37] The DFT simulations carried out here suggest that the Li_2VO_2F structure possess a number of Li–O–Li bonds. Such bonds have been shown to be crucial for the occurrence of anionic redox reactions.[38]

4 | CONCLUSIONS

Local structural symmetries in disordered rock salt oxyfluoride Li_2VO_2F were studied by Raman spectroscopy supplemented by computations using DFT. The material possesses very specific SRO that are hidden in the corresponding conventionally analyzed diffraction patterns. Our DFT calculations suggest that Li_2VO_2F displays ordered cation and anion arrangements, as lithium ions preferentially are surrounded by fluoride anions, whereas vanadium ions are preferentially surrounded by oxygens. Furthermore, the cations tend to aggregate with their own species, that is, lithium and vanadium, respectively, form agglomerations. The Raman spectrum of chemically delithiated Li_xVO_2F also shows that the DRS structure is preserved upon delithiation and presents evidence of possible anionic redox reactions. These results display that Raman spectroscopy in combination with DFT calculations is a powerful tool in order to characterize ionic short-range order arrangements and thereby to estimate the anion redox reactions in Li-rich disordered rock salt materials.

ACKNOWLEDGEMENTS

This project has received funding from the European Union's Horizon 2020 research and innovation program under grant agreement no. 711792 (LiRichFCC). We also acknowledge STandUP for energy. Infrastructure provided by the Swedish National Infrastructure for Computing (SNIC) is gratefully acknowledged. This work contributes to the research performed at CELEST (Center for Electrochemical Energy Storage Ulm-Karlsruhe).

REFERENCES

[1] N. Nitta, F. Wu, J. T. Lee, G. Yushin, *Mater. Today* **2015**, *18*, 252.
[2] R. J. Clément, Z. Lun, G. Ceder, *Energy Environ. Sci.* **2020**, *13*, 345.
[3] R. Chen, S. Ren, M. Knapp, D. Wang, R. Witter, M. Fichtner, H. Hahn, *Adv. Energy Mater.* **2015**, *5*. 1401814
[4] M. A. Cambaz, B. P. Vinayan, H. Euchner, R. E. Johnsen, A. A. Guda, A. Mazilkin, Y. V. Rusalev, A. L. Trigub, A. Gross, M. Fichtner, *ACS Appl. Mater. Interfaces* **2018**, *10*, 21957.
[5] R. Chen, S. Ren, M. Yavuz, A. A. Guda, V. Shapovalov, R. Witter, M. Fichtner, H. Hahn, *Phys. Chem. Chem. Phys.* **2015**, *17*, 17288.
[6] N. Pereira, F. Badway, M. Wartelsky, S. Gunn, G. G. Amatucci, *J. Electrochem. Soc.* **2009**, *156*, A407.
[7] W. Choi, A. Manthiram, *Electrochem. Solid-State Lett.* **2006**, *9*, A245.
[8] I. Källquist, A. J. Naylor, C. Baur, J. Chable, J. Kullgren, M. Fichtner, K. Edström, D. Brandell, M. Hahlin, *Chem. Mater.* **2019**, *31*, 6084.
[9] C. Baur, I. Källquist, J. Chable, J. H. Chang, R. E. Johnsen, F. Ruiz-Zepeda, J.-M. Ateba Mba, A. J. Naylor, J. M. Garcia-Lastra, T. Vegge, F. Klein, A. R. Schür, P. Norby, K. Edström, M. Hahlin, M. Fichtner, *J. Mater. Chem. A* **2019**, *7*, 21244.
[10] H. Ji, A. Urban, D. A. Kitchaev, D.-H. Kwon, N. Artrith, C. Ophus, W. Huang, Z. Cai, T. Shi, J. C. Kim, H. Kim, G. Ceder, *Nat. Commun.* **2019**, *10*, 592.
[11] R. J. Clément, D. Kitchaev, J. Lee, G. Ceder, *Chem. Mater.* **2018**, *30*, 6945.
[12] W. H. Kan, B. Deng, Y. Xu, A. K. Shukla, T. Bo, S. Zhang, J. Liu, P. Pianetta, B.-T. Wang, Y. Liu, G. Chen, *Chem* **2018**, *4*, 2108.
[13] M. A. Jones, P. J. Reeves, I. D. Seymour, M. J. Cliffe, S. E. Dutton, C. P. Grey, *Chem. Commun.* **2019**, *55*, 9027.
[14] C. M. Julien, A. Mauger, *AIMS Mater. Sci.* **2018**, *5*, 650.
[15] E. Flores, P. Novák, E. J. Berg, *Front. Energy Res.* **2018**, *6*, 1.
[16] C. Baur, J. Chable, F. Klein, V. S. K. Chakravadhanula, M. Fichtner, *ChemElectroChem* **2018**, *5*, 1484.
[17] G. Kresse, J. Furthmüller, *Comput. Mater. Sci.* **1996**, *6*, 15.
[18] G. Kresse, J. Furthmüller, *Phys. Rev. B* **1996**, *54*, 11169.
[19] G. Kresse, J. Hafner, *Phys. Rev. B* **1993**, *47*, 558.
[20] G. Kresse, J. Hafner, *Phys. Rev. B* **1994**, *49*, 14251.
[21] J. P. Perdew, K. Burke, M. Ernzerhof, *Phys. Rev. Lett.* **1996**, *77*, 3865.
[22] J. P. Perdew, K. Burke, M. Ernzerhof, *Phys. Rev. Lett.* **1997**, *78*, 1396.
[23] S. L. Dudarev, G. A. Botton, S. Y. Savrasov, C. J. Humphreys, A. P. Sutton, *Phys. Rev. B* **1998**, *57*, 1505.
[24] P. E. Blöchl, *Phys. Rev. B* **1994**, *50*, 17953.
[25] A. Fonari and S. Stauffer, Vasp_raman.Py, https://Github.Com/Raman%2010Sc/VASP/, **2013**.
[26] K. Momma, *F. Izumi* **2011**, 1272.
[27] C. Baur, M.-E. Lăcătuşu, M. Fichtner, R. E. Johnsen, *ACS Appl. Mater. Interfaces* **2020**, *12*, 27010.
[28] M. I. Aroyo, J. M. Perez-Mato, C. Capillas, E. Kroumova, S. Ivantchev, G. Madariaga, A. Kirov, H. Wondratschek, *Zeitschrift für Krist. - Cryst. Mater.* **2006**, *221*, 15.
[29] R. E. Ruther, A. F. Callender, H. Zhou, S. K. Martha, J. Nanda, *J. Electrochem. Soc.* **2014**, *162*, A98.
[30] J. Chable, C. Baur, J. H. Chang, S. Wenzel, J. M. García-Lastra, T. Vegge, *J. Phys. Chem. C* **2020**, *124*, 2229.
[31] D. Chen, X. Xiong, B. Zhao, M. A. Mahmoud, M. A. El-Sayed, M. Liu, *Adv. Sci.* **2016**, *3*. 1500433
[32] P. Tarte, J. Preudhomme, *Spectrochim. Acta Part a Mol. Spectrosc.* **1970**, *26*, 747.
[33] J. Preudhomme, P. Tarte, *Spectrochim. Acta Part a Mol. Spectrosc.* **1971**, *27*, 961.
[34] P. Shvets, O. Dikaya, K. Maksimova, A. Goikhman, *J. Raman Spectrosc.* **2019**, *50*, 1226.

[35] X. Wang, Y. Huang, D. Ji, F. Omenya, K. Karki, S. Sallis, L. F. J. Piper, K. M. Wiaderek, K. W. Chapman, N. A. Chernova, M. S. Whittingham, *J. Electrochem. Soc.* **2017**, *164*, A1552.

[36] X. Li, Y. Qiao, S. Guo, Z. Xu, H. Zhu, X. Zhang, Y. Yuan, P. He, M. Ishida, H. Zhou, *Adv. Mater.* **2018**, *30*. 1705197

[37] X. Li, Y. Qiao, S. Guo, K. Jiang, M. Ishida, H. Zhou, *Adv. Mater.* **2019**, *31*. 1807825

[38] M. Li, T. Liu, X. Bi, Z. Chen, K. Amine, C. Zhong, J. Lu, *Chem. Soc. Rev.* **2020**, *49*, 1688.

SUPPORTING INFORMATION

Additional supporting information may be found online in the Supporting Information section at the end of this article.

How to cite this article: Mozhzhukhina N, Kullgren J, Baur C, et al. Short-range ordering in the Li-rich disordered rock salt cathode material Li_2VO_2F revealed by Raman spectroscopy. *J Raman Spectrosc*. 2020;1–7. https://doi.org/10.1002/jrs.5953